Available online at www.sciencedirect.com
SCIENCE DIRECT®
Chemical Physics Letters 407 (2005) 159–165
CHEMICAL PHYSICS LETTERS
www.elsevier.com/locate/cplett

Influence of isotherm inflection on the diffusivities of C5–C8 linear alkanes in MFI zeolite

R. Krishna *, J.M. van Baten

Van't Hoff Institute for Molecular Sciences, University of Amsterdam Nieuwe Achtergracht 166, 1018 WV Amsterdam, The Netherlands

Received 13 February 2005; in final form 17 March 2005
Available online 7 April 2005

Abstract

Molecular Dynamics (MD) simulations have been carried out to determine the Maxwell–Stefan (M–S) diffusivities $Đ_i$ for linear alkanes with 5, 6, 7 and 8 carbon atoms in MFI zeolite at 433 K for a range of molecular loadings Θ. The dependence of the MS diffusivities $Đ_i$ on the loading Θ was found to exhibit strong inflection behaviour; this is caused by the inflection in the corresponding sorption isotherm. The $Đ_i - \Theta$ dependence follows the trend suggested by Krishna et al. [R. Krishna, J.M. van Baten, D. Dubbeldam, J. Phys. Chem. B 108 (2004) 14820]. The inflection behaviour also extends to diffusivities in binary mixtures.

1. Introduction

Zeolites are widely used as catalysts and adsorbents in a variety of applications in the chemical and petrochemical industries [1] and it is generally accepted that the Maxwell–Stefan (M–S) diffusion formulation provides a convenient and general framework that can be used in practice [2–4]. For single component diffusion of species i, the M–S formulation

$$\mathbf{N}_i = -\rho\Theta_i Đ_i \frac{1}{RT}\nabla_{T,p}\mu_i \equiv -\rho\Theta_{i,\mathrm{sat}} Đ_i \frac{\theta_i}{RT}\nabla_{T,p}\mu_i \qquad (1)$$

relates the flux $\mathbf{N}_i$ to the chemical potential gradient $\nabla_{T,p}\mu_i$. In Eq. (1), Θ_i is molecular loading expressed say in molecules per unit cell, $\Theta_{i,\mathrm{sat}}$ is the saturation loading, $\theta_i \equiv \Theta_i/\Theta_{i,\mathrm{sat}}$ is the fractional occupancy, ρ is the zeolite framework density expressed as the number of unit cells per m^3, R is the gas constant, T is the temperature, and $Đ_i$ is the M–S diffusivity. For solving practical problems involving single component diffusion it is necessary to have information on the variation of the M–S diffusivity $Đ_i$ with the fractional occupancy θ_i. Several publications in recent years have used molecular dynamics (MD) simulations to determine M–S diffusivities of pure components and mixtures in a variety of zeolite topologies [4–11]; these data are in reasonably good agreement with experimental data [12–14] in a few cases. Often, the $Đ_i$ is observed to decrease linearly with occupancy

$$Đ_i = Đ_i(0)(1-\theta_i). \qquad (2)$$

More generally, molecule–molecule interactions, zeolite topology and connectivity cause a variety of more complex dependences to be observed [15,16]. Interestingly, for diffusion of CF_4 and ethane in MFI zeolite, MD simulations show an *inflection* in the loading dependence of $Đ_i$ [12,14], caused by an inflection in the sorption isotherm [17,18].

In our earlier study using configurational-bias Monte Carlo (CBMC) simulations, we had shown that the sorption isotherms for linear alkanes with 6, 7 and 8 carbon atoms in MFI zeolite exhibit inflection behaviour, due a variety of reasons [19]. It may therefore be expected that the M–S diffusivity $Đ_i$ would also show inflection behaviour. The first major objective of the

* Corresponding author. Fax: + 31 20 5255604.
E-mail address: r.krishna@uva.nl (R. Krishna).

0009-2614/$ - see front matter © 2005 Elsevier B.V. All rights reserved.
doi:10.1016/j.cplett.2005.03.073

present communication is to investigate, with the aid of MD simulations, the loading dependence of the M–S diffusivities of *n*C5 (*n*-pentane), *n*C6 (9-hexane), *n*C7 (*n*-heptane) and *n*C8 (*n*-octane) in MFI zeolite and to test the validity of the model developed earlier [17]. The second major objective is to examine to what extent the isotherm inflection behaviour will influence the diffusion in *binary* mixtures. For this purpose we performed MD simulations with *n*C5/*n*C6 and *n*C7/*n*C8 mixtures for a variety of loadings.

2. CBMC and MD simulations

CBMC and MD Simulations have been carried out for *n*C5, *n*C6, *n*C7 and *n*C8 alkanes in MFI (all silica silicalite-1, topology shown in Fig. 1a) at 433 K; the crystallographic data are available elsewhere [20,21]. For both adsorption and diffusion simulations we use the united atom model. The zeolite framework is considered to be rigid. We consider the CH_x groups as single, chargeless interaction centers with their own effective potentials. The beads in the chain are connected by harmonic bonding potentials. A harmonic cosine bending potential models the bond bending between three neighboring beads, a Ryckaert–Bellemans potential controls the torsion angle. The beads in a chain separated by more than three bonds interact with each other through a Lennard–Jones potential. The Lennard–Jones potentials are shifted and cut at 12 Å. Pure component adsorption isotherms for alkanes were determined using CBMC simulations. The CBMC simulation details, along with the force fields have been given in detail in other publications [22]. The simulation box consists of $2\times2\times2$ unit cells and periodic boundary conditions were employed. It was verified that the size of the simulation box was large enough to yield reliable data on adsorption and diffusion.

Diffusion in a system of N molecules is simulated using Newton's equations of motion until the system properties, on average, no longer change in time. The Verlet algorithm is used for time integration. The energy drift of the entire system is monitored to ensure that the time steps taken were not too large. A time step of 1 fs was used in all simulations. For each simulation, initializing CBMC moves are used to place the molecules in the domain, minimizing the energy. Next, a fixed number of MD initialization cycles are performed, at which velocities are scaled each cycle to the temperature. This is followed by a fixed number of equilibrium MD cycles. During the equilibrium cycles, statistics are not updated, and the velocities are no longer scaled at each cycle. After a fixed number of initialization and equilibrium steps, the MD simulation production cycles start. For every cycle, the statistics for determining the mean square displacements (MSDs) are updated. The MSDs are determined for time intervals ranging from 2 fs to 1 ns. In order to do this, an order-N algorithm, as detailed in Chapter 4 of Frenkel and Smit [23] is implemented. The details on how diffusivities are determined from the MSDs are also to be found in Frenkel and Smit [23] and elsewhere [11,21]. The Nosé–Hoover thermostat is used to main constant temperature conditions.

In the earlier publications of Sanborn and Snurr [10] and Skoulidas et al. [7], the Onsager matrix $[L]$, defined by $(\mathbf{N}) = -[L]\,(\nabla\mu)$ were determined from the MSDs using linear response theory. From the view point of determination of the M–S diffusivities, we find it much more convenient to define a matrix $[\Delta]$

$$\mathbf{N}_i = -\frac{\rho}{k_B T}\Theta_i \Sigma_{j=1}^{n} \Delta_{ij} \nabla\mu_j;\ \ i = 1, 2...n \tag{3}$$

and determine the elements of this matrix from

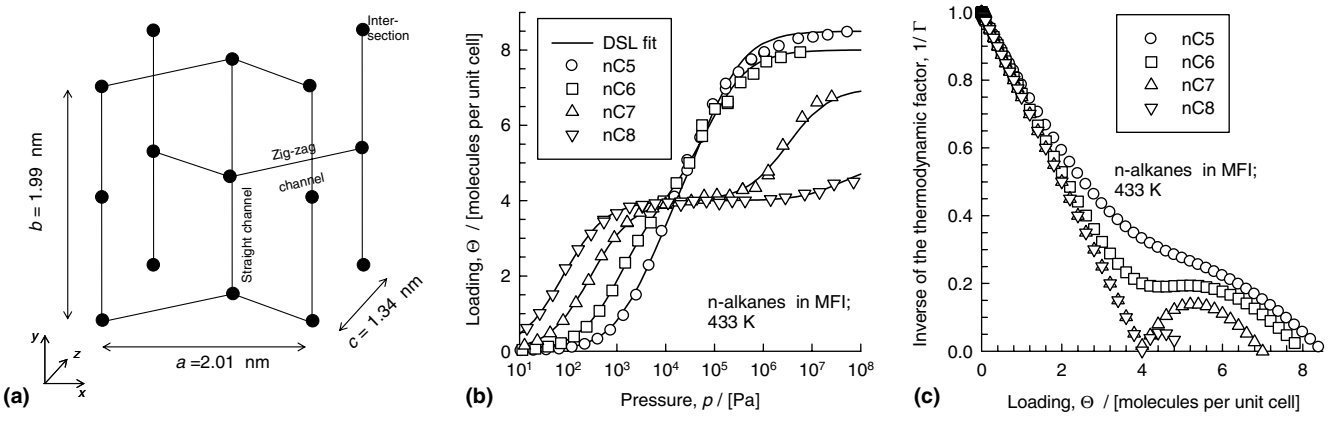

Fig. 1. (a) Schematic of the MFI topology. (b) CBMC simulations (open symbols) of the sorption isotherms for *n*C5, *n*C6, *n*C7 and *n*C8 in MFI at 433 K. The continuous solid lines represent the dual-site Langmuir fits of the isotherms with the parameter values specified in Table 1. (c) The inverse of the thermodynamic factor, $1/\Gamma$, as function of the molecular loading, using calculations following Eq. (13).

$$\Delta_{ij} = \frac{1}{6}\lim_{\Delta t\to\infty}\frac{1}{N_i}\frac{1}{\Delta t}\left\langle\left(\sum_{l=1}^{N_i}(\mathbf{r}_{l,i}(t+\Delta t)-\mathbf{r}_{l,i}(t))\right)\cdot\left(\sum_{k=1}^{N_j}(\mathbf{r}_{k,j}(t+\Delta t)-\mathbf{r}_{k,j}(t))\right)\right\rangle. \quad (4)$$

In this expression N_i and N_j represent the number of molecules of species i and j, respectively, and $\mathbf{r}_{l,i}(t)$ is the position of molecule l of species i at any time t. From the definition $\Theta_i = N_i/\rho V$, where V is the volume of the simulation box, we see that $\rho\Theta_i\Delta_{ij} = L_{ij}k_BT$ and therefore the Onsager reciprocal relations $L_{ij} = L_{ji}$ lead to

$$\Theta_i\Delta_{ij} = \Theta_j\Delta_{ji}. \quad (5)$$

For single component diffusion, $n = 1$, Δ_{11} can be identified with the M–S, or 'corrected' diffusivity $Đ_1$. Eq. (3) can be re-written as

$$(\mathbf{N}) = -\rho[\Delta][\Gamma](\nabla\Theta). \quad (6)$$

The matrix of thermodynamic correction factors $[\Gamma]$ is defined by

$$\frac{\Theta_i}{k_BT}\nabla\mu_i \equiv \sum_{j=1}^{n}\Gamma_{ij}\nabla\Theta_j;\quad \Gamma_{ij} = \frac{\Theta_i}{\Theta_j}\frac{\partial\ln p_i}{\partial\ln\Theta_j};\ i,j = 1,2\ldots n, \quad (7)$$

where p_i represents the partial pressure (or, more strictly, the fugacity) of component i in the bulk fluid phase. The Γ_{ij} can be calculated from knowledge of the multicomponent sorption isotherms [3,4].

The self-diffusivities, $D_{i,\text{self}}$ were computed by analyzing the mean square displacement of each component in the usual manner

$$D_{i,\text{self}} = \frac{1}{6N_i}\lim_{\Delta t\to\infty}\frac{1}{\Delta t}\left\langle\left(\sum_{l=1}^{N_i}(\mathbf{r}_{l,i}(t+\Delta t)-\mathbf{r}_{l,i}(t))^2\right)\right\rangle. \quad (8)$$

3. Simulation results

The CBMC simulations for the adsorption isotherms are shown in Fig. 1b. The isotherms conform very closely to the dual-site Langmuir isotherm

$$\Theta(p) \equiv \Theta_A + \Theta_B;\quad \Theta_A = \frac{\Theta_{\text{sat,A}}b_Ap}{1+b_Ap};\quad \Theta_B = \frac{\Theta_{\text{sat,B}}b_Bp}{1+b_Bp} \quad (9)$$

with fitted DSL model parameters as specified in Table 1. In Eq. (9) b_A and b_B represent the DSL model parameters expressed in Pa^{-1} and the subscripts A and B refer to two sorption sites within the MFI structure, with different sorption capacities and sorption strengths. The $\Theta_{\text{sat,A}}$ and $\Theta_{\text{sat,B}}$ represent the saturation capacities of sites A and B, respectively. We can rewrite Eq. (9) as a quadratic expression in terms of the pressure:

$$(\Theta_{\text{sat,A}}+\Theta_{\text{sat,B}}-\Theta)b_Ab_Bp^2 + ((\Theta_{\text{sat,A}}-\Theta)b_A + (\Theta_{\text{sat,B}}-\Theta)b_B)p - \Theta = 0. \quad (10)$$

The pressure for a given total loading Θ within the zeolite can be obtained from the physically feasible solution to Eq. (9)

$$p = \frac{1}{2}\left(\frac{\sqrt{\beta^2+4\alpha\Theta}-\beta}{\alpha}\right) = \frac{1}{2\alpha}(\sqrt{\beta+4\alpha\Theta}-\beta), \quad (11)$$

where

$$\alpha = (\Theta_{\text{sat,A}}+\Theta_{\text{sat,B}}-\Theta)b_Ab_B;$$
$$\beta = (\Theta_{\text{sat,A}}-\Theta)b_A + (\Theta_{\text{sat,B}}-\Theta)b_B. \quad (12)$$

Krishna et al. [17,18] have shown that for many molecule-zeolite topologies the loading dependence of the M–S diffusivity $Đ_i$ is dictated by the inverse of the thermodynamic factor defined by Eq. (7). Using Eq. (7), we can obtain the inverse of the thermodynamic factor Γ in the convenient form

$$\frac{1}{\Gamma} = x_A(1-\theta_A) + x_B(1-\theta_B);\quad x_A = \frac{\Theta_A}{\Theta};$$
$$x_B = \frac{\Theta_B}{\Theta};\quad \theta_A = \frac{\Theta_A}{\Theta_{\text{A,sat}}};\quad \theta_B = \frac{\Theta_B}{\Theta_{\text{B,sat}}}, \quad (13)$$

where x_A and x_B are the fractions of the total loading Θ present in sites A and B. Eqs. (11) and (12) allow $1/\Gamma$ to be calculated explicitly as a function of the total loading Θ. Fig. 1c shows that the inflection behaviour of $1/\Gamma$ increases in strength as the chain length increases.

Table 1
Dual-site Langmuir parameters, and zero-loading diffusivities for *n*-alkanes in MFI at 433 K

	Dual-site Langmuir parameters				Zero-loading diffusivities	
	b_A	$\Theta_{\text{sat,A}}$	b_B	$\Theta_{\text{sat,B}}$	$Đ(0)$	$Đ_y(0)$
*n*C5	2.33×10^{-4}	4.0	1.36×10^{-5}	4.5	0.63	1.4
*n*C6	8.35×10^{-4}	4.0	1.35×10^{-5}	4.0	0.5	1.2
*n*C7	3.41×10^{-3}	4	3.1×10^{-7}	3	0.55	1.3
*n*C8	1.28×10^{-2}	4	2.36×10^{-8}	1	0.55	1.3

The saturation capacity Θ_{sat} has the units of molecules per unit cell. The Langmuir parameters b_i have the units of Pa^{-1}. The diffusivities have the units of 10^{-8} $\text{m}^2\,\text{s}^{-1}$.

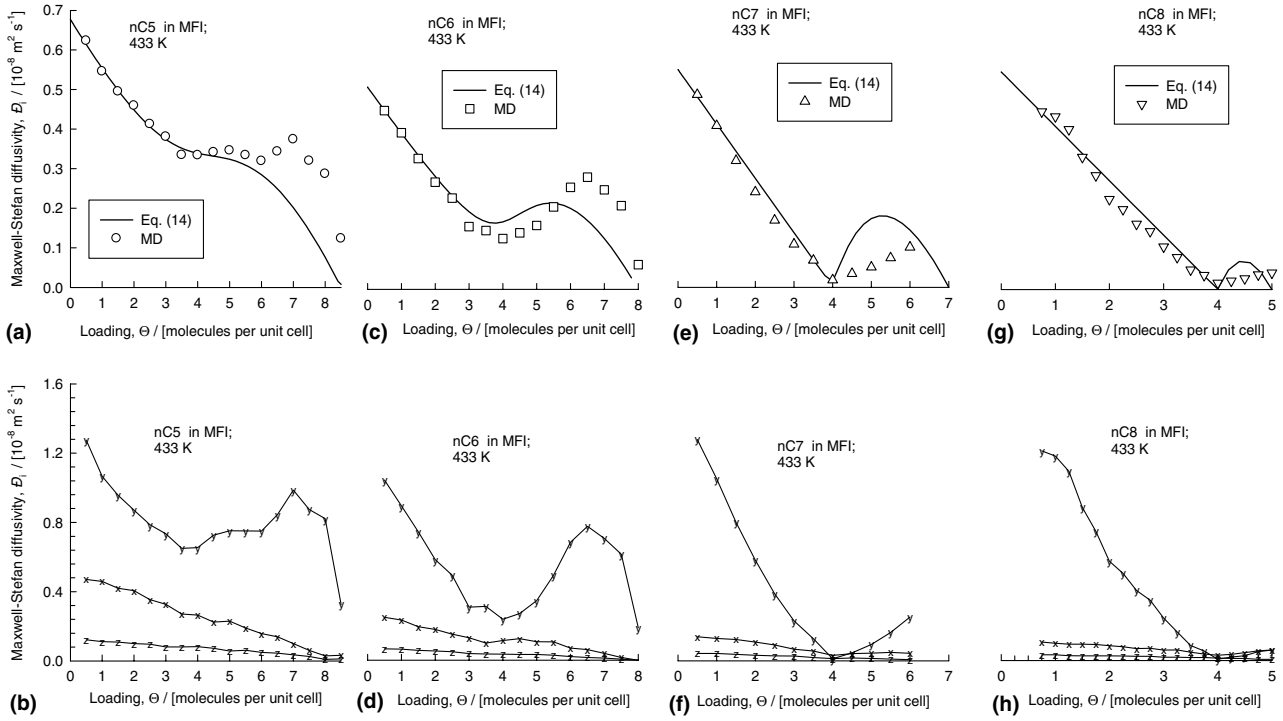

Fig. 2. MD Simulation results of the loading dependence of the M–S diffusivities $Đ_i$ for *n*-alkanes in MFI at 433 K. In the top row the MD simulated values of $Đ_i$ (denoted by open symbols) are compared with the calculations following Eq. (14), shown by continuous solid lines. In the bottom row the M–S diffusivities in the *x*-, *y*-, and *z*-directions are shown as a function of loading.

The MD simulation results for $Đ_i$ are shown in the top row in Fig. 2. For all *n*-alkanes we observe an inflection in the $Đ_i$ at a loading $\Theta = 4$ molecules per unit cell, corresponding to the number of intersections in one unit cell (see Fig. 1a). For *n*C7 and *n*C8 the $Đ_i$ reduces to virtually zero at $\Theta = 4$ before increasing when the loading exceeds 4. The bottom row in Fig. 2 gives data on the M–S diffusivities in *x*-, *y*- and *z*-directions (as indicated in Fig. 1a). For all *n*-alkanes we note that the inflection behaviour is predominantly in the *y*-direction, i.e., for diffusion along the straight channels; the M–S diffusivities in the *x*- and *z*-directions decrease almost monotonously with increased loading. Assuming that beyond the point of inflection, the molecular traffic is only along the straight channels, Krishna et al. [17] derived the following expression:

$$Đ = Đ(0)x_A(1 - \Theta_A/\Theta_{sat,A}) + Đ_y(0)x_B(1 - \Theta_B/\Theta_{sat,B}), \quad (14)$$

where $Đ(0)$ is the zero-loading orientation averaged M–S diffusivity, and $Đ_y(0)$ is the zero-loading diffusivity for transport along the straight channels; the values of these diffusivities are listed in Table 1. The calculations following Eq. (14) are shown by the continuous solid lines in Figs. 2a,c,e,g. We see that Eq. (14) provides a reasonably good description of the loading dependence of the M–S diffusivities for all four *n*-alkanes investigated.

Another interesting point to note in the data presented in Fig. 2 is that *n*C7 and *n*C8 appear to diffuse equally fast in MFI.

Let us now turn to diffusion in binary *n*-alkane mixtures. We performed simulations for 75–25, 50–50, and 25–75 binary mixtures of *n*C5 and *n*C6 at various loadings; the data on $Đ_{ij}$ and the self-diffusivities $Đ_{i,self}$ are shown in Fig. 3. In Fig. 3 the pure component data are also included for comparison with mixture diffusion data. We note first that both $Đ_{ij}$ and $Đ_{i,self}$ show an inflection in the loading dependence at $\Theta = 4$. The $Đ_{11}$ decreases significantly when the proportion of *n*C6 in the mixture increases, suggesting that the more mobile species is retarded significantly in the presence of the slower moving species. On the other hand the $Đ_{22}$ is hardly influenced by the mixture composition, suggesting that the less mobile *n*C6 is almost uninfluenced by the presence of the more mobile *n*C5.

For a loading of $\Theta = 3.75$, MD simulations were carried out for a variety of *n*C5/*n*C6 mixture compositions; the results are shown in Figs. 4a,b. Increasing the proportion of *n*C5 in the mixture has the effect of increasing both $Đ_{ij}$ and $Đ_{i,self}$ an expected result.

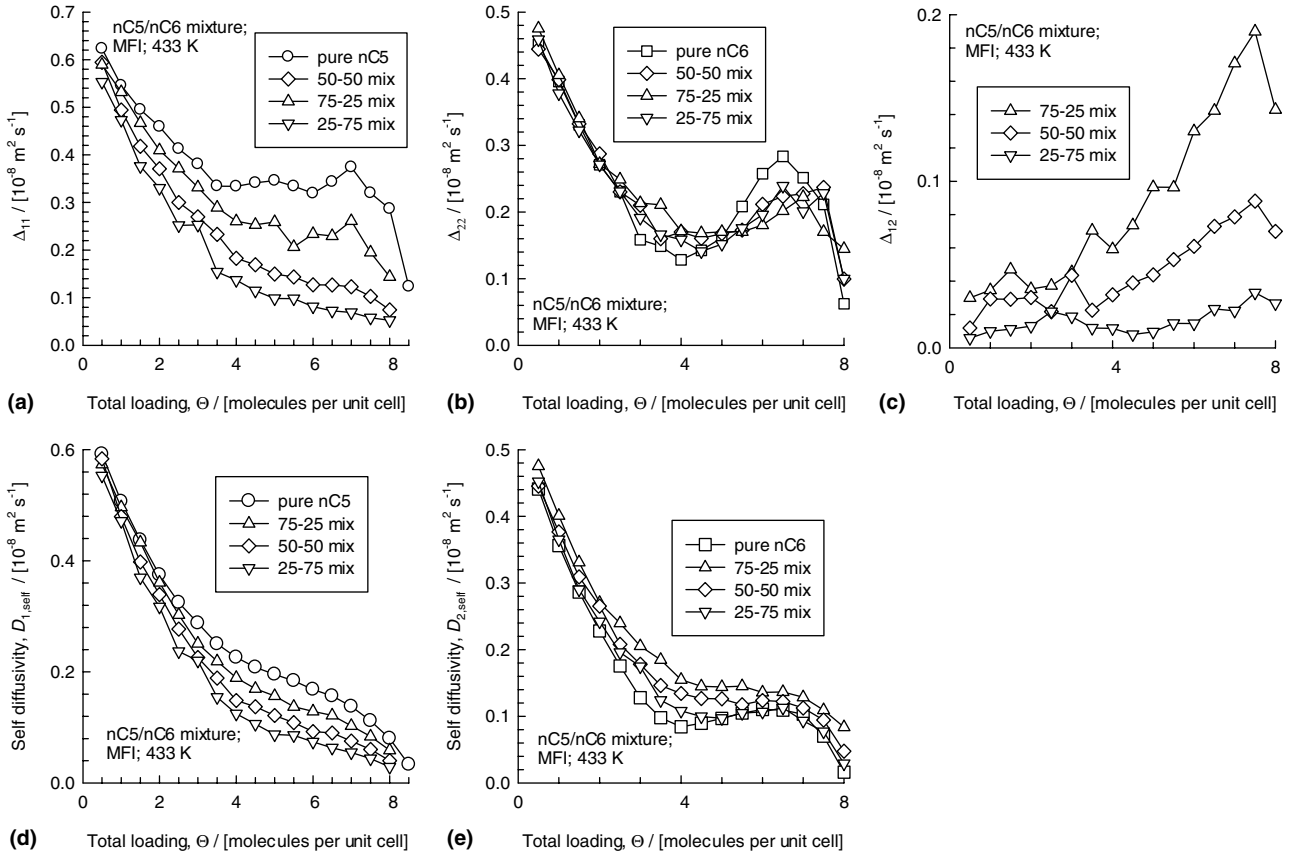

Fig. 3. MD Simulation data for (a,b,c) Δ_{ij} and (d,e) $D_{i,\text{self}}$ in binary mixtures (pure *n*C5, 75–25, 50–50, 25–75, pure *n*C6) of *n*C5/*n*C6 in MFI at 433 K at various loadings.

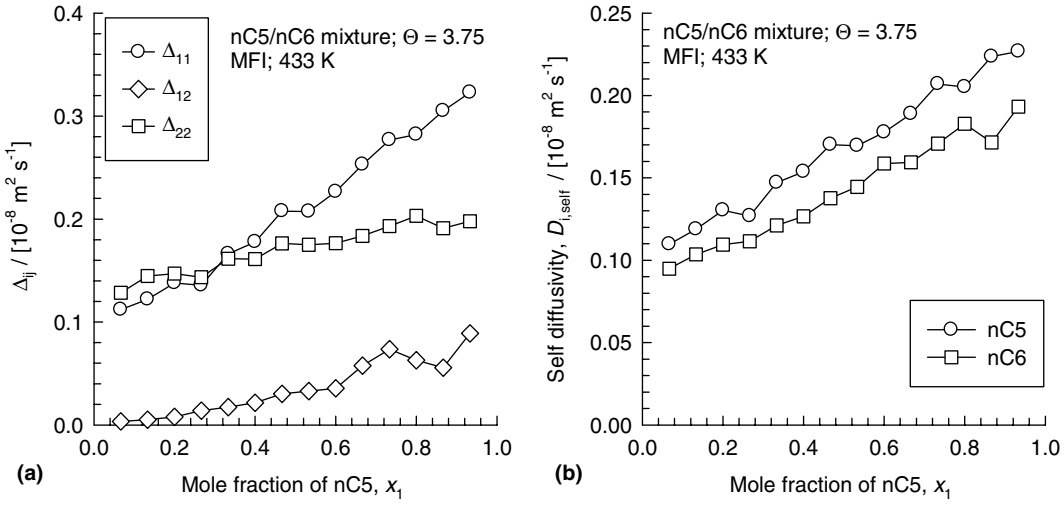

Fig. 4. Influence of mixture composition on (a) Δ_{ij} and (b) $D_{i,\text{self}}$ in binary mixtures of *n*C5/*n*C6 in MFI at 433 K at a loading $\Theta = 3.75$ molecules per unit cell.

The MD simulation results for *n*C7/*n*C8 mixtures are shown in Fig. 5. Since the pure component mobilities are nearly the same (see Fig. 2), the Δ_{ij} and $D_{i,\text{self}}$ values in the mixture have nearly the same values as for the corresponding pure components, and a strong infection in the diffusivities is observed at a loading of $\Theta = 4$.

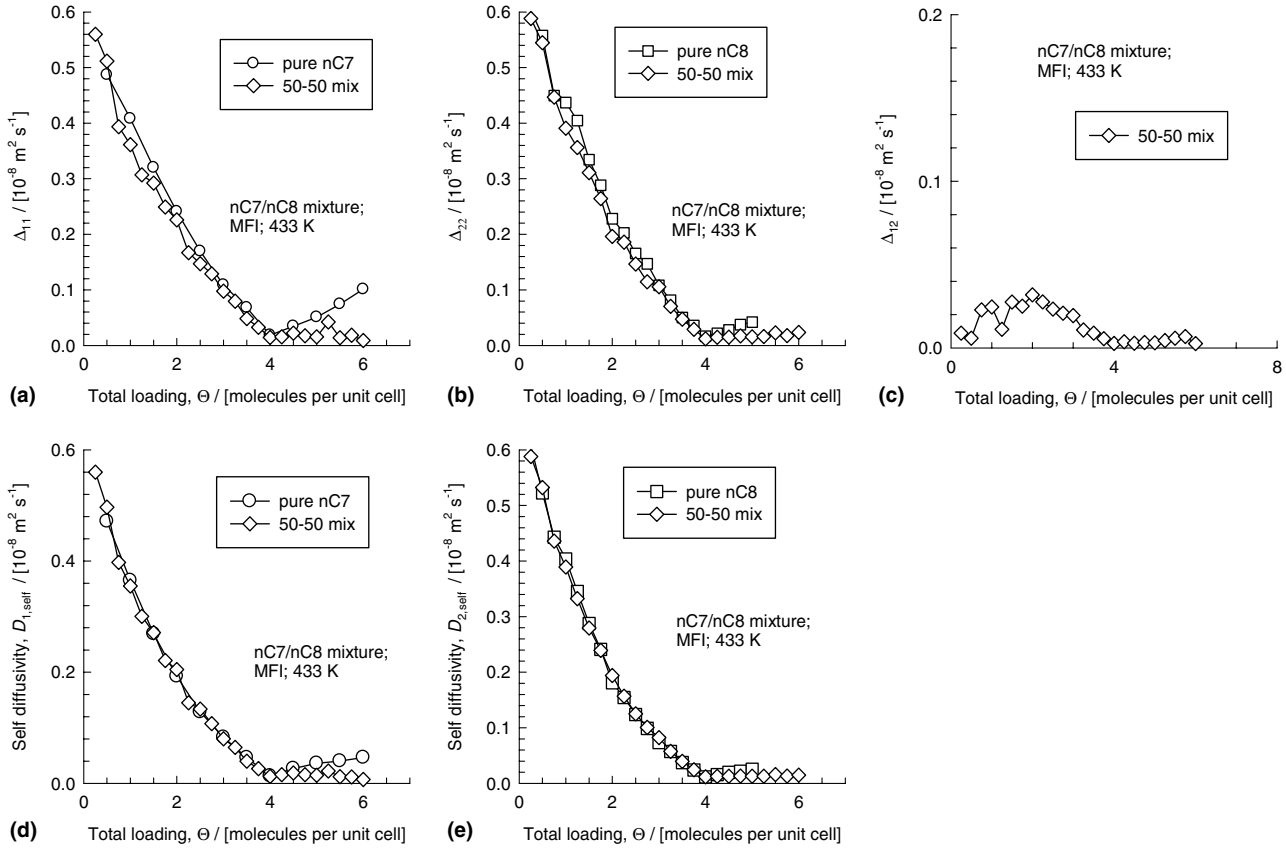

Fig. 5. MD Simulation data for (a,b,c) Δ_{ij} and (d,e) $D_{i,\mathrm{self}}$ in binary mixtures (pure *n*C7, 50–50, pure *n*C8) of *n*C7/*n*C8 in MFI at 433 K at various loadings.

4. Conclusions

The loading dependence of the M–S diffusivity $Đ_i$ of *n*-alkanes with 5, 6, 7 and 8 carbon atoms in MFI was investigated with the aid of MD simulations. In all cases the $Đ_i$ exhibits inflection behaviour at a loading of $\Theta = 4$, corresponding to the isotherm inflection. The loading dependence of $Đ_i$ is reasonably well described by the model of Krishna et al. [17], Eq. (14), in which it is assumed that for loading in excess of that at the inflection point, the molecular traffic is predominantly along the straight channels of MFI.

The inflection characteristics are also reflected in mixture diffusion.

It is necessary to obtain experimental verification of the inflection behaviour as evidenced in our theoretical investigation.

Acknowledgements

R.K. acknowledges two grants: *Programmasubsidie* and TOP subsidy from the Netherlands Foundation for Fundamental Research (NWO-CW) for the development of novel concepts in reactive separations technology and for intensification of reactors. We gratefully acknowledge D. Dubbeldam, S. Calero, T.J.H. Vlugt, E. Beerdsen and B. Smit for providing the CBMC and MD simulation codes. We acknowledge NWO/NCF for provision of high performance computing resources.

References

[1] J. Kärger, D.M. Ruthven, Diffusion in Zeolites and Other Microporous Solids, John Wiley, New York, 1992.
[2] F.J. Keil, R. Krishna, M.O. Coppens, Rev. Chem. Eng. 16 (2000) 71.
[3] R. Krishna, R. Baur, Sep. Purif. Technol. 33 (2003) 213.
[4] A.I. Skoulidas, D.S. Sholl, R. Krishna, Langmuir 19 (2003) 7977.
[5] E.J. Maginn, A.T. Bell, D.N. Theodorou, J. Phys. Chem. 97 (1993) 4173.
[6] A.I. Skoulidas, D.S. Sholl, J. Phys. Chem. A 107 (2003) 10132.
[7] A.I. Skoulidas, T.C. Bowen, C.M. Doelling, J.L. Falconer, R.D. Noble, D.S. Sholl, J. Membr. Sci. 227 (2003) 123.
[8] S. Chempath, R. Krishna, R.Q. Snurr, J. Phys. Chem. B 108 (2004) 13481.
[9] H. Ramanan, S.M. Auerbach, M. Tsapatsis, J. Phys. Chem. B 108 (2004) 17171.
[10] M.J. Sanborn, R.Q. Snurr, Sep. Purif. Technol. 20 (2000) 1.
[11] R. Krishna, J.M. van Baten, J. Phys. Chem. B 109 (2005) 6386.

[12] H. Jobic, A.I. Skoulidas, D.S. Sholl, J. Phys. Chem. B 108 (2004) 10613.
[13] G.K. Papadopoulos, H. Jobic, D.N. Theodorou, J. Phys. Chem. B 108 (2004) 12748.
[14] C. Shang-Shan, H. Jobic, M. Plazanet, D.S. Sholl, Chem. Phys. Lett. (2005) (in press).
[15] A.I. Skoulidas, D.S. Sholl, J. Phys. Chem. B 106 (2002) 5058.
[16] R. Krishna, D. Paschek, R. Baur, Micropor. Mesopor. Mater. 76 (2004) 233.
[17] R. Krishna, J.M. van Baten, D. Dubbeldam, J. Phys. Chem. B 108 (2004) 14820.
[18] R. Krishna, J.M. van Baten, Chem. Eng. Technol. 28 (2005) 160.
[19] T.J.H. Vlugt, W. Zhu, F. Kapteijn, J.A. Moulijn, B. Smit, R. Krishna, J. Am. Chem. Soc. 120 (1998) 5599.
[20] C. Baerlocher, L.B. McCusker, Database of zeolite structures. Available from: <http://www.iza-structure.org/databases/>, 12 October 2004.
[21] J.M. van Baten, R. Krishna, MD Simulations of diffusion in zeolites, University of Amsterdam. Available from: <http://ct-cr4.chem.uva.nl/md/>, 1 November 2004.
[22] D. Dubbeldam, S. Calero, T.J.H. Vlugt, R. Krishna, T.L.M. Maesen, B. Smit, J. Phys. Chem. B 108 (2004) 12301.
[23] D. Frenkel, B. Smit, Understanding Molecular Simulations: From Algorithms to Applications, Academic Press, San Diego, 2002.